Moderately Concentrated Solutions of Polystyrene. 3. Viscoelastic Measurements at the Flory Θ Temperature

J. O. Park† and G. C. Berry*

Department of Chemistry, Carnegie-Mellon University, Pittsburgh, Pennsylvania 15213.
Received October 14, 1988

ABSTRACT: Linear and nonlinear viscoelastic properties are reported for solutions of polystyrene in moderately concentrated solutions in dioctyl phthalate at the Flory Θ temperature. Measurements include the linear recoverable creep compliance and the nonlinear viscosity. The solutions are for concentrations c in the entanglement regime ($\phi M_w > M_C$) but have $[\eta]c$ in the range 4–30. The results are compared with the properties of solutions of polystyrene in good solvents, including data reported here for solutions in tricresyl phosphate. Effects on the linear viscosity η_0 and steady-state recoverable compliance $R_0(s)$ are discussed and shown to have a simpler dependence on concentration at the Flory Θ temperature than in good solvents if $c < c_s$. Effects on the nonlinear viscosity are small if the shear rate κ is expressed in the reduced form $\eta_0 R_0^{(s)}\kappa$.

Introduction

Linear and nonlinear viscoelastic properties are reported below for solutions of polystyrene in moderately concentrated solutions in bis(2-ethylhexyl)phthalate (dioctyl phthalate, DOP) at the Flory Θ temperature; the latter is equal to 22 °C.[1] In addition, some results are given for solutions of polystyrene in DOP for $T > \Theta$ and for solutions of polystyrene in tri-*m*-tolyl phosphate (tricresyl phosphate, TCP); the latter is a thermodynamically good solvent for polystyrene; see below.

In part 1 of this series, the (linear) viscosity η_0 of moderately concentrated solutions of polystyrene was fitted by the relation[2]

$$\eta_0 = \eta^{(R)}(c/\rho)^n E(\alpha_C^2 cM/\rho M_C) \tag{1a}$$

$$\eta^{(R)} = N_A X\zeta/6 \tag{1b}$$

where M is the molecular weight, c and ρ are the solute concentration and density (wt/vol), respectively, M_C is a constant, α_C is the ratio of the mean-square radius of gyration at concentration c to the value $R_{G,0}^2$ at infinite dilution and the Flory Θ temperature, n is in the range 0–0.5 (see below), and $\eta^{(R)}$ is the Rouse viscosity. Here, ζ is the segmental friction factor of a chain segment of length l, and $X = \alpha_C^2 cMC/6M_L^2$, with M_L the mass per unit contour length L of the chain, and C a constant given by $C = 6R_{G,0}^2/Ll$ in the limit of large L. For many chains, $X_C = \rho M_C C/6M_L^2$ is a constant (400×10^{-17} in cgs units) if l is the length per chain atom,[3] providing an estimate for M_C in terms of C, etc. The function E may be represented as[4,5]

$$E(X/X_C) = [1 + (X/X_C)^{2.4\epsilon}]^{1/\epsilon} \tag{2}$$

where use of $\epsilon = 2$ will provide a fit to most data, such that $\eta_0 \propto \alpha_C^2 cM$ for $X < X_C$ and $\eta_0 \propto (\alpha_C^2 cM)^{3.4}$ for $X > X_C$.

The dependence of α_C on c obtained in neutron-scattering studies[6] may be expressed in the form[5]

$$\alpha_C^2 = \begin{cases} \alpha_0^2[1 + (k\hat{c})^2]^{-s/2}; & c < c_s \\ 1; & c \geq c_s \end{cases} \tag{3}$$

where $\hat{c} = (N_A R_G^3/M)c$, with R_G the root-mean-square radius of gyration at infinite dilution, $\alpha_0 = R_G/R_{G,0}$, c_s is a system-dependent constant, k is a constant (see below), and $s \approx (2\mu - 1)/3\mu$, with $\mu = 3\nu - 1$ and $\nu = \partial \ln R_G/\partial \ln M$; μ is about equal to $\partial \ln [\eta]/\partial \ln M$ and $\hat{c} = [\eta]c/6.8$ for high molecular weight flexible chains, with $[\eta]$ the intrinsic viscosity. The constant k may be estimated from the condition that the intramolecular monomer density is about equal to the overall monomer density (i.e., cN_A/M) when α_C begins to deviate from α_0. With that criterion, $k\hat{c} \approx [\eta]c$,[5,7] and $c_s \approx [\eta]^{-1}\alpha_0^{2/s}$.

In part 1, the segmental friction factor ζ was expressed in the form

$$\zeta = K\eta_s \exp(b_T w) \tag{4}$$

for moderately concentrated solutions, where η_s is the solvent viscosity, w is the solute weight fraction, and K and b_T are constants, the latter dependent on the temperature T. The relation of eq 4 to free-volume treatments of ζ is discussed below.

The empirical behavior expressed by eq 1–3 is similar in form to a theoretical result given by Muthukumar and Edwards,[8] for the case with $X < X_C$, though that treatment gives $n = 1$, which appears to be larger than the experimental value. Theoretical estimates of $E(X/X_C)$ differ from eq 2. Thus, one estimate gives[9]

$$E(X/X_C) = 15(X/X_C)^2 \tag{5}$$

for undiluted polymer ($c = \rho$) for $X \gg X_C$, whereas another treatment gives the result[10]

$$E(X/X_C) \approx 9.6[1 - (X_C/X)^{1/2}]^3(X/X_C)^2 \tag{6}$$

in the same limit. The latter expression is numerically similar to eq 2 over a range of large X/X_C.

Equations 1–4 provide a consistent representation of η_0 in poor solvents ($T \approx \Theta$) or good solvents and reveal the lack of simple scaling laws for η_0. For example, whereas α_C scales with $[\eta]c$, η_0 depends also on $cM/\rho M_C$ (which does not scale with $c[\eta]$) and on the essentially molecular weight independent but concentration dependent ζ. In this study we will investigate linear and nonlinear viscoelastic behavior for moderately concentrated solutions of polystyrene under conditions with $\alpha_C = 1$ (i.e., $T = \Theta$) and in good solvents, for which $\alpha_0 > 1$. As in previous work[11] on moderately concentrated solutions of polystyrene in TCP, results will be discussed in terms of the BKZ-type single-integral constitutive equation[12]

$$\sigma_M(t) = \sum \eta_i \tau_i^{-2} \int_0^\infty [\Delta\gamma(t,u)]^M F[\Delta\gamma(t,u)] \exp(-u/\tau_i)\, du \tag{7}$$

where $\Delta\gamma(t,u) = \gamma(t) - \gamma(t-u)$, with γ the strain, and F is a function known reasonably well; see below. With eq 7, $\sigma_1(t)$ is the shear stress $\sigma(t)$ and $\sigma_2(t)$ is the first normal stress difference $\nu(t)$, and it is assumed that the linear shear relaxation modulus $G(t)$ may be expressed in the form

$$G(t) = \sum \eta_i \tau_i^{-1} \exp(-t/\tau_i) \tag{8}$$

with τ_i the ith relaxation time, and the weight factors η_i normalized such that $\eta_0 = \sum \eta_i$. Application of eq 7 to

† Present address: Lucky Central Research Institute, Chungnam, Korea.

0024-9297/89/2222-3022$01.50/0

Table I
Parameters for the Solutions Studied

polym	solvt	wt fractn polym	temp range, °C	$10^{-5}M_w$	$c[\eta]^a$	$cM_w/\rho M_C$	log η/($\eta_s(\phi M_w)^{3.4}$) (22 °C)^c	$R_0^{(N)}/R^{(R)d}$	$R_0^{(s)}/R^{(R)d}$
PC3	TCP	0.25	25.0–60.0	4.11	25.5	3.50	−11.95		0.97
		0.35	24.8–75.0		35.8	4.85	−11.03		0.90
		0.45	60.5–90.5		44.4	6.16	−10.36		0.68
PC6	TCP	0.10[b]		8.60	17.4	2.98	−14.00		1.23[b]
		0.123	27.0		20.9	3.67			1.26
		0.171	4.6–25.0		29.6	5.07	−13.13		1.03
		0.25[b]			43.0	7.33	−12.06		0.49[b]
		0.40[b]			67.9	11.6	−10.53		
		0.55[b]			92.1	15.7	−8.586		0.23[b]
		0.70[b]			116	19.8	−3.462		0.19[b]
PC3	DOP	0.25	22.0	4.11	12.9	3.06	−12.32		1.20
		0.35	22.0		18.2	4.34	−11.01	0.027	0.85
		0.41	22.0		21.4	5.25	−10.46	0.22	0.81
		0.45	22.0		23.6	5.62	−10.16	0.20	0.58
		0.55	22.0		29.2	6.93	−9.372	0.17	0.60
D500	DOP	0.02	22.0	71.0	4.20	4.16	−14.60		
		0.03	22.0–32.0		5.86	6.26	−14.61		1.33
		0.04	22.0–41.5		8.39	8.33	−13.89		1.10

[a] $[\eta]$ equal to 89.0 and 149 mL/g for PC3 and PC6 in TCP (22 °C), respectively, and 51.5 and 214 mL/g for PC3 and D500 in DOP (22 °C), respectively. [b] From ref 14. [c] η_s is 0.0561 Pa·s for DOP (22 °C) and 0.0674 Pa·s for TCP (22 °C). [d] $R^{(R)} = 2M/5cRT$.

compute nonlinear functions is discussed below. Values of η_i and τ_i may be determined by several methods, including study of $G(t)$ or the linear creep compliance $J(t)$. In the latter case, the τ_i and η_i may be computed from $G(t)$ calculated from the convolution integral[11,13]

$$\int_0^t ds\, J(t-s)\, G(s) = t \tag{9}$$

In the use of eq 9 it is convenient to express $J(t)$ in terms of η_0 and the retardation times λ_i and weights r_i as

$$J(t) = R(t) + t/\eta_0 \tag{10a}$$

$$R(t) = R(\infty) - [R(\infty) - R(0)]\textstyle\sum r_i \exp(-t/\lambda_i) \tag{10b}$$

where $\sum r_i = 1$, $R(\infty)$ is the value of $R(t)$ for large t, and $R(0)$ is the "instantaneous" value of $R(t)$; the latter is effectively fixed by the short time response of the equipment used. For a fluid, $R(\infty)$ is the steady-state recoverable compliance, here denoted $R_0^{(s)}$, the subscript indicating linear behavior ($R_0^{(s)}$ is often denoted J_e^0 [ref 13]). Methods to determine the r_i and λ_i from experimental data on $R(t)$ and to compute the η_i and τ_i from these by the use of eq 8 are discussed elsewhere.[11]

Experimental Section

Materials. Three polystyrenes prepared by anionic polymerizations were used in this study: PC3a and PC6a (Pressure Chemical Co., Pittsburgh, PA) and D-500 (Duke Scientific Corp., Palo Alto, CA). Polymers were dried under vacuum (10^{-5} Torr) for 2–3 days before use. Technical grade tricresyl phosphate (Fisher Chemical Co.) and dioctyl phthalate (Eastman Chemical Products) were used. Both were held under vacuum at 80 °C for 3 days before use to remove water. Solvents were maintained dry following procedures described elsewhere.[11] The systems studies are given in Table I, including estimates for $c[\eta]$ and $cM_w/\rho M_C$. In the former case, $[\eta]$ is calculated from

$$[\eta] = K_\eta (M_w/m_0)^\mu \tag{11}$$

with m_0 the molar weight of a monomeric unit (m_0 = 104 for polystyrene); μ = 0.5 and K_η = 0.82 mL/g for solutions in DOP at 22 °C,[1] and μ = 0.7 and $K_\eta \approx$ 0.27 mL/g for solutions in TCP; the latter are estimates based on limited data[14] and may not apply for M_w much different from that used here. The value of M_C was taken to be 31 200,[3] and ρ for polystyrene is given by[15]

$$\rho_{25}/\rho = 0.824 + 10^{-4}(5.9 + 691/M_n)T \tag{12}$$

where ρ_{25} = 1.074 g/mL is the density for large M at 25 °C and T is the absolute temperature (in kelvins).

Dried polymer and solvents were mixed by weight at the desired composition, and reagent grade benzene was added to bring the final polymer concentration to about 1–2%. Dissolution was effected in a closed container over several days, with slow stirring using a magnetic stirring bar. The solutions were then filtered through a Teflon membrane, 30–60-μm pore size (Chemplast, Inc., Wayne, NJ), and the benzene evaporated under vacuum at 60 °C until the solution reached a constant weight.

Where needed (e.g., to compute c from w), the density of polymer solutions was computed on the assumption of volume additivity, with

$$\rho/\rho_{25} = 1.262 - 8.77 \times 10^{-4}T \tag{13}$$

for TCP,[14] where ρ_{25} = 0.943 g/mL, and ρ = 0.9835 for DOP at 22 °C.[1]

Rheological Measurements. Measurements were carried out with either a Rheometrics RMS-7200 spectrometer or the CMU-II rheometer constructed in our laboratory; the latter is described in detail elsewhere.[16] The Rheometrics apparatus was used principally for studies of stress growth with a ramp strain history ($\gamma(t) = \kappa t$ for $t > 0$), stress relaxation following cessation of steady flow, stress relaxation following a step strain, and dynamic mechanical experiments with an imposed sinusoidal strain. The CMU-II rheometer was used for studies of the creep compliance, the recoverable strain on cessation of steady flow, and dynamic mechanical experiments with an imposed sinusoidal stress using methods described elsewhere.[16,17] A Birnboim data acquisition system and correlator was used to implement sinusoidal experiments in either case.

All data were obtained by using a cone-and-plate geometry, with α = 0.033 rad and R = 2.02 cm for the CMU-II rheometer, and α = 0.035 rad and R = 1.25 cm for the Rheometrics apparatus, where α is the angle between the cone and plate and R is the radius.

Results

The linear recoverable creep compliance $R(t)$ and the storage shear compliance $J'(\omega)$ are shown in Figure 1 for solutions of PC3a and D-500 in DOP at the Flory temperature (22 °C). Corresponding plots of the creep compliance $J(t)$ are not given since $J(t)$ is accurately given by eq 10a using the $R(t)$ in Figure 1 and the η_0 given in Table I. The absolute dynamic shear compliance $J^{(d)}(\omega)$ followed the Riande–Markovitz relation[18,19]

$$[J(t)]_{wt=1} \approx J^{(d)}(\omega) = \{[J'(\omega)^2] + [J''(\omega)^2]\}^{1/2} \tag{14}$$

and $J'(\omega)$, given by[13,19,20]

$$J'(\omega) = R_0^{(s)} - \omega \int_0^\infty [R_0^{(s)} - R(u)] \sin \omega u\, du \tag{15}$$

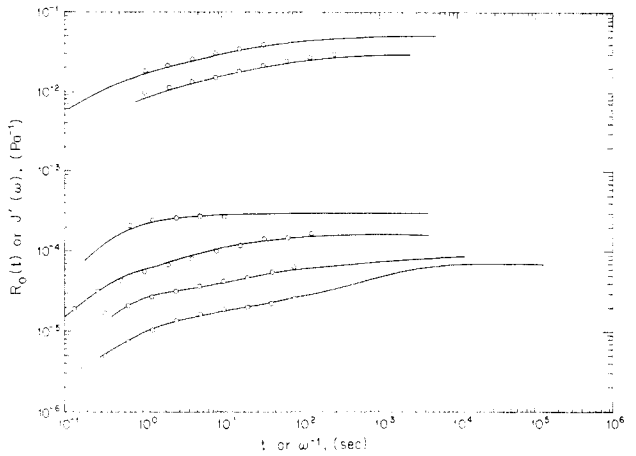

Figure 1. Bilogarithmic plots of the recoverable compliance $R(t)$ versus t and the storage compliance $J'(\omega)$ versus ω^{-1} for several solutions of polystyrene in DOP at the Flory Θ temperature. In descending order from the top: D-500, 3%; D-500, 4%; PC3a, 25%; PC3a, 35%; PC3a, 45%; PC3a, 55%. The solid curves give $R(t)$ and the circles give $J'(\omega)$.

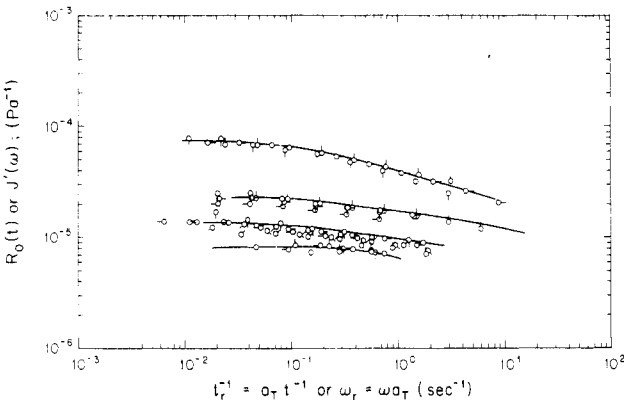

Figure 2. As in Figure 1 for solutions of polystyrene PC3a in TCP, with 17.1%, 25%, 35%, and 45% polymer from top to bottom. The temperatures are given as follows, with pips rotating clockwise from straight up: 17.1%, *4.6*, 13.0, 25.0 °C; 25%, *25.0*, 40.0, 50.0 °C; 35%, 24.9, 32.2, *41.4*, 46.4, 49.8, 60.0, 75.0 °C; 45%, 60.5, 75.0, *90.5* °C. The factor a_T is given by eq 17, with T_R indicated by the italicized temperature for each concentration.

is about equal to $[R(t)]_{wt=1}$ for the range of ω studied. With the use of eq 10b

$$J'(\omega) = R_0^{(s)} - [R_0^{(s)} - R(0)]\sum r_i(\omega\lambda_i)^2/[1 + (\omega\lambda_i)^2] \quad (16)$$

Comparison of eq 10b and 16 reveals the source for the approximation $J'(\omega) \approx [R(t)]_{wt=1}$ since $x^{-2}[1 + x^{-2}]^{-1} - \exp(-x)$ is close to zero for most x and never exceeds 0.2. Data on $J'(\omega)$ are shown in Figure 2 for solutions of PC3a in TCP for a range of temperatures—the reduced frequency $a_T\omega$ is used to superpose the data at different temperatures, where

$$a_T = \tau_C(T)/\tau_C(T_R) \quad (17)$$

with $\tau_C(T)$ the time constant $\eta_0 R_0^{(s)}$ at temperature T, and T_R an arbitrary reference temperature.

Similar data on $R(t)$ and $J'(\omega)$ are given in Figure 1 for solutions of D-500 in DOP. As seen in Table I, $\phi M_w/M_C$ is at least as large as the values used for solutions of the other polymers studied, but both the volume fraction $\phi = c/\rho$ and $c[\eta]$ are much smaller. The data on D-500 cover a narrow temperature range, with $\Theta \leq T/K < \Theta + 20$. Superposed reduced plots are obtained over this range by use of the reduced time t/a_T and frequency $a_T\omega$.

Values of $R_0^{(s)}$ and $R_0^{(N)}$ are given in Table I, normalized by the Rouse recoverable compliance $2M/5cRT$. Values

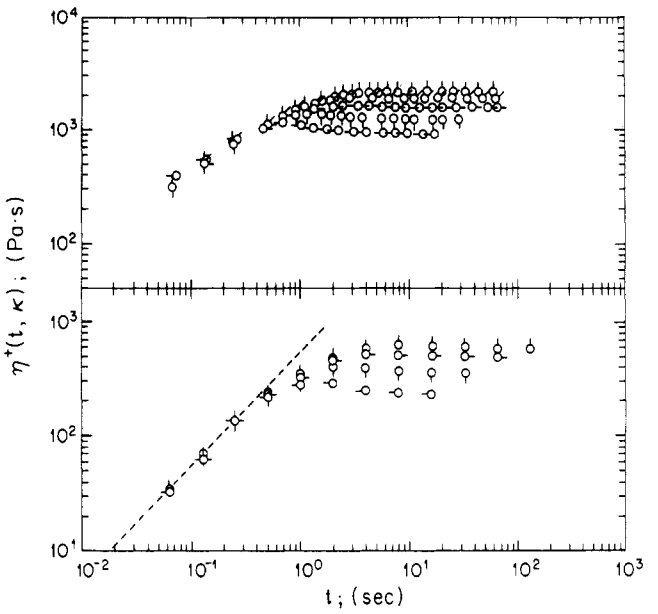

Figure 3. Bilogarithmic plots of the stress growth function $\eta^+(t,\kappa)$ versus t for two solutions of polystyrene at several values of κ. Upper: PC3a in DOP at 25 °C, 25%, with κ/s^{-1} equal to 0.177, 0.493, 0.945, 1.89, and 3.49 as the pips rotate clockwise from straight up. Lower: PC3a in TCP at 22 °C, 25%, with κ/s^{-1} equal to 0.239, 0.478, 0.956, and 1.91 as the pips rotate clockwise from straight up.

of η_0 determined as the asymptotic value of $[\partial J(t)/\partial t]^{-1}$ for $t > \tau_C$ are given in Table I in the form $\eta_0/\eta_s(\phi M_w)^{3.4}$. Here, $\eta_s = 0.0561$ Pa·s at 22 °C and $\partial \ln \eta_s/\partial T^{-1} = 5275$ K for DOP; the temperature dependence of η_s for TCP is discussed below, but $\eta_s = 0.0674$ Pa·s at 22 °C. Data from the literature[14,21-23] for solutions of polystyrenes in TCP and DOP are included in Table I for comparison.

As shown in Figure 3, typical nonlinear effects were observed in ramp strain experiments with solutions of PC3a in either DOP or TCP. Thus, for strain κt less than some value γ', $\sigma(t)/\kappa$ is independent of κ. For larger κt, $\sigma(t)$ exhibits a maximum at a characteristic strain γ^+ that appears to be independent of κ. Similar behavior was found with a solution of PC6a in TCP. Values of γ' and γ^+ are given in Table II, where it is seen that both are independent of temperature and that γ^+ is independent of ϕ, but that γ' decreases with increasing ϕ.

Another manifestation of nonlinear behavior is shown in Figure 4 for data on the nonlinear shear compliance $G(t,\gamma)$ as a function of the strain γ; $G(t,\gamma)$ was determined as $\sigma(t)/\gamma$, where $\sigma(t)$ is the stress at time t following a strain jump γ. As with other materials,[9] the data obtained here may be represented by the relation

$$G(t,\gamma) = G(t)\, F(|\gamma|) \quad (18)$$

over the limited range of t and $|\gamma|$ studied, where F is the function appearing in eq 7. The function $F(|\gamma|)$ is shown in Figure 5 for a solution of PC3a in DOP, where it is seen that $F(|\gamma|)$ may be represented by a simple relation used elsewhere[11,19] to estimate the nonlinear behavior of polymer solutions:

$$F(|\gamma|) \approx \exp\left(m\left(\frac{|\gamma| - \gamma'}{\gamma''}\right)\right) \quad (19)$$

where m is zero for $|\gamma| < \gamma'$ and unity otherwise. Use of eq 19 in eq 7 gives $\gamma'' = \gamma^+$.

The stress relaxation following steady flow was determined as a function of the shear rate κ for solutions of PC3a in TCP. As seen in Figure 6 the stress relaxation function $\eta^-(t,\kappa)$, defined as the stress at time t after ces-

Table II
Critical Strain Parameters

polym	solvt	wt fract polym	vol fract polym	temp, °C	γ'^a	γ^{+b}
PC3a	DOP	0.25	0.233	22.0	1.04	2.46
		0.35	0.330	22.0		2.61
		0.41	0.400	22.0	0.60	2.23
		0.55	0.527	22.0	0.60	2.45
PC3a	TCP	0.25	0.266	25.0	1.03	2.52
			0.266	40.0	0.96	2.49
			0.265	60.0		2.51
		0.35	0.369	31.6	0.91	2.52
			0.369	41.4	0.96	2.50
			0.369	46.4	0.92	2.47
			0.369	49.8	0.92	2.51
			0.368	60.0		2.50
			0.367	75.0		2.49
		0.45	0.470	60.5	0.60	2.53
			0.469	75.0	0.62	2.55
			0.469	90.5	0.60	2.51
PC6a	TCP	0.171	0.184	4.6	1.34	2.58
			0.184	13.0		2.46

$^a\gamma' = \kappa t'$, where t' is the time above which the stress growth function exhibits departure from linear viscoelastic behavior. $^b\gamma^+ = \kappa t^+$, where t^+ is the time at which the stress reaches its maximum value in deformation at constant shear rate.

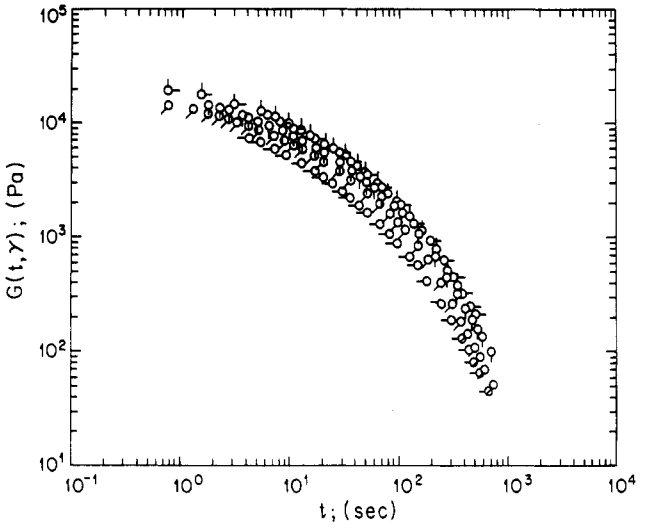

Figure 4. Bilogarithmic plots of $G(t,\gamma)$ versus t for a solution of PC3a in DOP, 41%, at the Flory Θ temperature, for five values of $|\gamma|$: 0.108, 0.195, 0.74, 1.27, and 2.36 as the pips rotate clockwise from straight up.

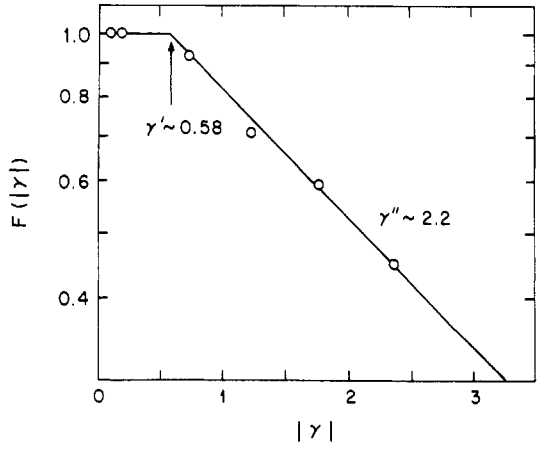

Figure 5. Semilogarithmic plot of $F(|\gamma|) = G(t,\gamma)/G(t,0)$ versus $|\gamma|$ for the data in Figure 4.

sation of steady flow at shear rate κ, divided by κ, was found to reduce to a single function when plotted as $\eta^-(t,\kappa)/\eta_\kappa$ versus $t/w^2\eta_\kappa$, where η_κ is the nonlinear steady-state

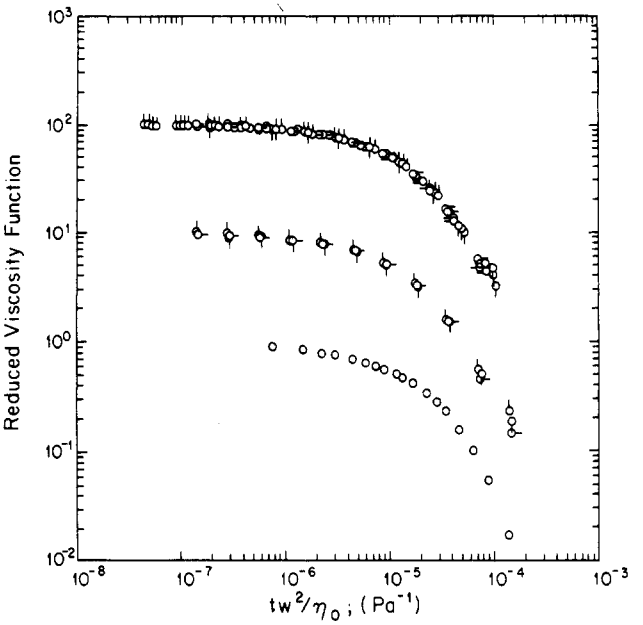

Figure 6. Bilogarithmic plots of the $\eta^-(t,\kappa)/\eta_\kappa$ versus w^2t/η_κ for several solutions of polystyrene. Here η_κ is the steady-state viscosity at rate of strain κ. Upper: Limiting behavior at small κ for PC3a in TCP, 35%, at 2.48, 31.6, 41.4, and 46.4 °C as the pips rotate clockwise from straight up. Ordinate multiplied by 100. Middle: Data for PC3a in TCP, 35%, at 31.6 °C for κ/s^{-1} equal to 0.0203, 0.0281, and 0.0306 as pips rotate clockwise from straight up. Ordinate multiplied by 10. Lower: Limiting behavior at small κ for PC3a in DOP, 45%, at the Flory Θ temperature.

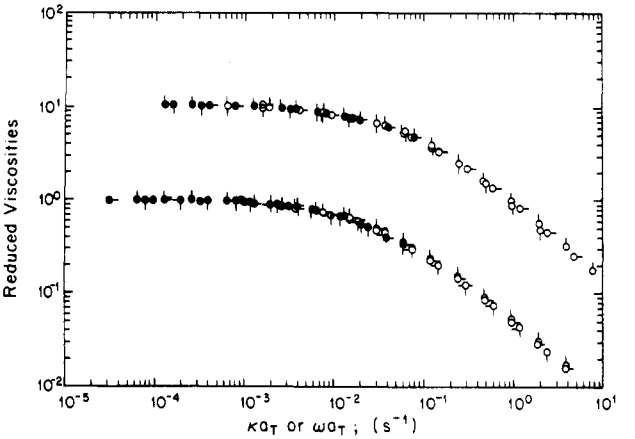

Figure 7. Bilogarithmic plots of viscosity functions for solutions of polystyrene D-500. Filled and unfilled circles are for η_κ/η_0 versus $a_T\kappa$ and $\eta^{(d)}(\omega)/\eta_0$ versus $a_T\omega$, respectively. Upper: Data are for 3% polymer in DOP, at 22.0, 25.3, and 32.9 °C as the pips rotate clockwise from straight up. Ordinate multiplied by 10. Lower: Data are for 4% polymer in DOP at 22.0, 27.5, 31.7, and 41.5 °C as the pips rotate clockwise from straight up.

viscosity of shear rate κ (see below).

The nonlinear steady-state viscosity η_κ was determined over a range of κ for several of the systems studied, with the results given in Figures 7 and 8. As with many polymers and their solutions, for solution of polystyrene in DOP the Cox–Merz approximation[19,24]

$$\eta_\kappa \approx [\eta^{(d)}(\omega)]_{\kappa=\omega} \tag{20}$$

provides a link between the nonlinear η_κ and the linear absolute dynamic viscosity $\eta^{(d)}(\omega)$, calculated as $[\omega J^{(d)}(\omega)]^{-1}$. In addition, the linear function $[\eta^-(t,0)]_{\kappa t=1}$ also approximates η_κ, as shown in Figure 8 (see below).

Discussion

Linear Viscoelastic Parameters. The linear creep and recovery behavior provide values for the viscosity η_0

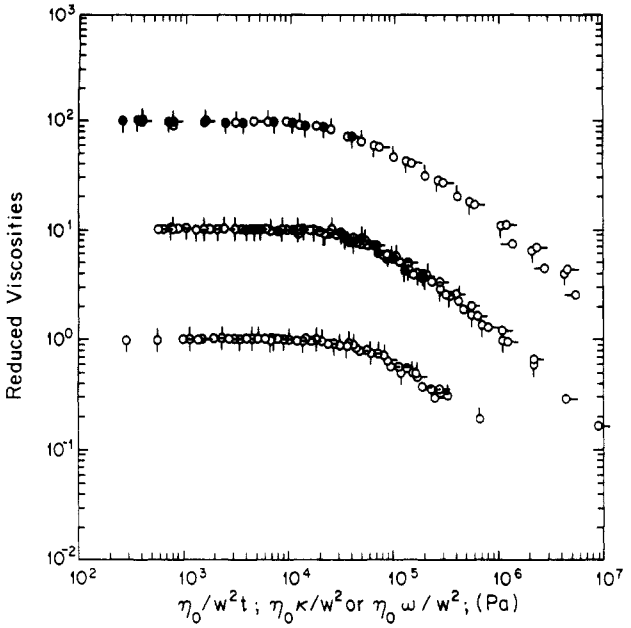

Figure 8. Bilogarithmic plots of viscosity functions for solutions of PC3a, with 25%, 35%, 45% and 55% polymer as the pips rotate clockwise from straight up. Upper: η_κ/η_0 versus $\kappa\eta_0/w^2$ and $\eta^{(d)}(\omega)/\eta_0$ versus $\omega\eta_0/w^2$ for filled and open circles, respectively, for solutions in DOP at the Flory Θ temperature. Ordinate multiplied by 100. Middle: η_κ/η_0 versus $\kappa\eta_0/w^2$ and $\eta^+(t,0)/\eta_0$ versus η_0/w^2t for filled and open circles, respectively, for solutions in TCP. Ordinate multiplied by 10. Lower: $\eta^{(d)}(\omega)/\eta_0$ versus $\omega\eta_0/w^2$ for solutions in TCP.

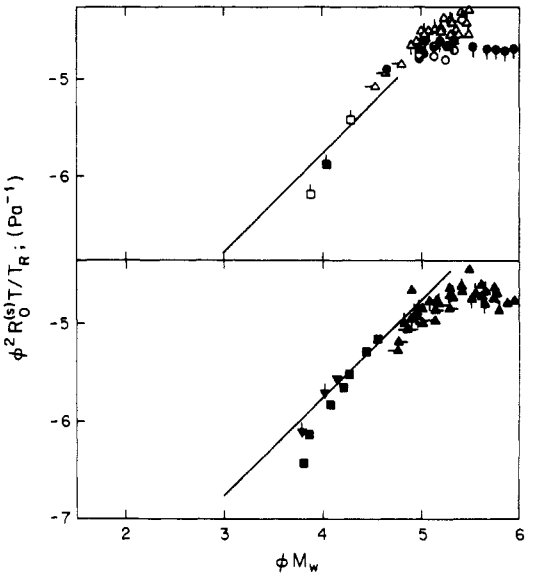

Figure 9. Bilogarithmic plots of $\phi^2R_0^{(s)}T/T_R$ versus ϕM_w for solutions of polystyrenes in DOP, TCP, α-chloronaphthalene, and aroclors; T_R is a reference temperature (295 K). The circles designate PC3a (no pip), PC6a (pip down), and D-500 (pip up), for solutions in DOP at the Flory Θ temperature (unfilled) and TCP (filled). Some of these data are taken from ref 14 (see Table I). The triangles are data from the literature[23] for three values of M_w: 2.06×10^7 (no pip), 8.42×10^6 (pip up), 4.48×10^6 (pip down), and 7.75×10^5 (pip left). In DOP (T = 30 °C, unfilled) and α-chloronaphthalene (T = 30 °C, filled). The squares are data from the literature[25] on solutions in DOP (unfilled) at the Flory Θ temperature, and aroclor at 25 °C (filled), for M_w equal to 8.2×10^4 (pip up) or 5.1×10^4 (no pip).

and steady-state recoverable compliance $R_0^{(s)}$ as discussed above. In addition, as seen in several of the examples, $R(t)$ (or $J'(\omega)$) is essentially independent of t over an intermediate range of t (typically, $1 < t/\tau_C < 10$) before increasing with increasing t (or decreasing ω) to reach its asymptotic value $R_0^{(s)}$ for large t (or small ω). The plateau value of $R(t)$ in the intermediate range is denoted $R_0^{(N)}$ to designate its connection to a pseudonetwork created by the entanglement constraints among the chains. For the data obtained here on solutions of PC3a in DOP with w = 0.35, 0.41, 0.45, and 0.55, $R_0^{(s)}/R_0^{(N)}$ is independent of concentration and equal to 3.3. Similar behavior is reported[14,21] for solutions of PC6a in TCP over the range $0.1 < \phi \leq 1$—$\phi M_w > M_C$ for the stipulated range in both cases.

As seen in Figure 9a, $\phi^2R_0^{(s)}T/T_R$ is essentially independent of ϕ, M_w, or solvent used (T_R being an arbitrary reference temperature), with the exception of the data on solutions of D-500 or DOP, for which $\phi^2R_0^{(s)}T/T_R$ is about twice as large as might be expected on the basis of the data or PC3a and PC6a. This deviation may be caused by molecular weight heterogeneity in the D-500 samples. Data reported in the literature for $R_0^{(s)}$ for polystyrene in DOP solution[23,25] and in TCP solutions[14] are included in Figure 9a for comparison, and values of $\phi^2R_0^{(s)}T/T_R$ in α-chloronaphthalene[23] and aroclor[26] are shown in Figure 9b.

For values of ϕM_w less than a critical value M_C' the behavior in Figure 9 gives $R_0^{(s)} \approx R^{(R)}$, where $R^{(R)}$ is the Rouse recoverable compliance, equal to $2M/5cRT$. For $\phi M_w > M_C'$, $R_0^{(s)}$ is less than $R^{(R)}$, and $\phi^2R_0^{(s)}$ is essentially independent of ϕ and M_w. In addition, in this regime, $R_0^{(s)}/R_0^{(N)}$ is a constant.

In the regime with $\phi M_w > M_C'$, $R_0^{(N)}$ and $R_0^{(s)}$ are determined by binary interactions, giving rise to the networklike behavior reflected in the parameter $R_0^{(N)}$. At the Flory Θ temperature the dependence on binary interactions among the Guassian chains leads to the result $R_0^{(N)} = M_C'R^{(R)}/M\phi$.[4,13,19] The same result is expected in a good solvent if $c > c_s$, such that $\alpha_C = 1$. As seen in Figure 9a, there is very little difference between $\phi^2R_0^{(s)}T/T_R$ for the solutions of PC3a in DOP and solutions of PC3a or PC6a in TCP, and $\phi^2R_0^{(s)}T/T_R$ is independent of ϕ for $\phi M_w > M_C' = 10^5$, or $M_C' \approx 3.2M_C$. For smaller ϕM_w, $\phi^2R_0^{(s)}T/T_R$ is proportional to ϕM_w until the concentration is small enough that $c[\eta] < 2$. For still smaller c, the behavior changes from that for a moderately concentrated solution to that for a dilute solution.[13] Computation with eq 3, putting $k\hat{c} = [\eta]c$ and $\alpha_0 \approx ([\eta]/[\eta]_0)^{1/3}$ shows that $c > c_s$, and $\alpha_C \approx 1$ for all of the solutions in TCP studied here.

In very good solvents (i.e., solutions with large α_0), binary interactions dominate the thermodynamic interactions, providing the basis for the suggested proportionality[27] between the network modulus $G_0^{(N)}$ ($=[R_0^{(N)}]^{-1}$) and the osmotic modulus $K_{os} = c\partial\,\Pi/\partial c$ in good solvents, where Π is the osmotic pressure. This proportionality does not obtain at the Flory Θ temperature since binary thermodynamic interactions are nil in that case, and K_{os} is dependent on nonpairwise additive ternary interactions in a moderately concentrated solution.[5] In a good solvent, with large second virial coefficient A_2, the osmotic pressure Π can be expressed in the form[5,7,27]

$$\Pi = (cRT/M)P(A_2Mc) \tag{21}$$

Thus, making use of the relation $A_2M \approx [\eta]$ in a very good solvent,[5,28] the proposed proportionality of $G_0^{(N)}$ to K_{os} gives

$$R_0^{(N)} \propto R^{(R)}[\partial cP([\eta]c)/\partial c]^{-1} \tag{22a}$$

$$R_0^{(N)} \propto \phi^{-(2+p)} \tag{22b}$$

Equation 22b results if it is assumed that $P([\eta]c)$ obeys the power law $P \propto ([\eta]c)^{1+p}$, in which case the stipulation that Π is independent of M in a moderately concentrated solution in a good solvent gives $p = (1 - \mu)/\mu$. Consequently, $\phi^2R_0^{(N)}$ is expected to be proportional to ϕ^{-p}, or

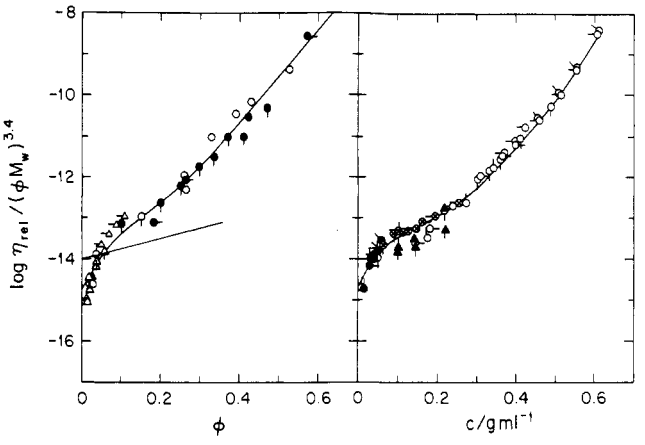

Figure 10. Bilogarithmic plots of η_0/η_s $(\phi M_w)^{3.4}$ versus ϕ for solutions of polystyrenes in DOP, TCP, and $\eta_0/c_s(cM_w)^{3.4}$ versus $c/(g\ mL^{-1})$ for solutions in toluene, *trans*-decalin, and aroclor; η_s is the solvent viscosity. Left: Symbols as designated in Figure 9 caption. The straight line gives the behavior reported in part 1 for solutions in cyclopentane. Right: Symbols designate solutions in aroclor (30 °C), unfilled circles;[26] toluene (25 °C), filled circles;[29] α-chloronaphthalene (20 or 50 °C), circles with cross;[23] and *trans*-decalin (25 °C), triangles.[29] The pips designate different molecular weights, in decreasing order of M_w as the pips rotate clockwise; see the original references.

$\phi^{-1/4}$ if $\mu = {}^4/_5$. The exponent p should decrease from ${}^1/_4$ to 0 as c exceeds c_s and the segment density approaches uniformity.[5,7,27] Furthermore, since the correspondence of K_{os} and $G_0^{(N)}$ rests on the predominance of binary interactions in Π, only the limiting result $p = {}^1/_4$ should be used in connection with eq 22, whereas at the Flory Θ temperature the form for $R_0^{(N)}$ should reduce to proportionality with ϕ^{-2} for $\phi M > M_C'$. A relation of the form

$$R_0^{(s)} = R^{(R)}\{1 + (\phi^{1+s}M/M_C')^{\epsilon}\}^{-1/\epsilon} \tag{23}$$

with $s = (2\mu - 1)/3\mu$ would have the desired behavior over a range of cM, in either very good solvents ($A_2M/[\eta] \approx 1$) or at the Flory Θ temperature ($A_2 = 0$); here, ϵ is an adjustable parameter greater than unity—this expression is not presented as exact but provides a means to interpolate between the desired limits.

For the data shown in Figure 9b for solutions of polystyrene in aroclor, $c < c_s$ for most of the data with $\phi M_w > M_C'$, and thermodynamic interactions are repulsive enough that $A_2M/[\eta]$ is expected to be a constant. The data for $\phi M_w > M_C'$ are scattered but could be consistent with $\phi^2 R_0^{(s)} \propto \phi^{-p}$, with $\mu = 0.7$ ($s = 0.19$).

The reduced relative viscosity is shown in Figure 10a for solutions in DOP and TCP—the data on solutions in TCP and DOP are augmented by results in ref 14 and 21 and ref 23, respectively. Similar data reported in the literature for solutions of polystyrene in other solvents are given in Figure 10b.[26,29] Combination of eq 1, 2, and 4 shows that $\eta_{rel}/(\phi M_w)^{3.4}$ should be proportional to $\phi^n \alpha_C^{6.8} \zeta(\phi)/\eta_s$. At the Flory Θ temperature, $\alpha_C = 1$, and $\phi^n\zeta(\phi)$ should depend only on ϕ for a given solvent and temperature. Similar behavior is expected if $c > c_s$ at all concentrations studied, as is the case with solutions in TCP studied here. Since η_s differs by only 18% for TCP and DOP at the temperatures of interest here, the correspondence of $\eta_{rel}/(\phi M_w)^{3.4}$ for solutions in these solvents is reasonable. The sharp increase in $\eta_{rel}/(\phi M_w)^{3.4}$ seen in Figure 10a for small ϕ is not in accord with the anticipated behavior for $\zeta(\phi)$ but is consistent with eq 1 with $n = {}^1/_2$. Similar behavior is reported in part 1 and has been predicted theoretically.[30] Thus $\eta_{rel}/\phi^{1/2}(\phi M_w)^{3.4}$ represents $\zeta(\phi)/\eta_s$ for the solutions in TCP and DOP studied.

The modified Vogel expression

$$\zeta = \zeta_{VOG} + \zeta_{ACT} \tag{24a}$$

$$\zeta_{VOG} = \zeta_0 \exp[1/\alpha(T - T_0)] \tag{24b}$$

$$\zeta_{ACT} = \zeta_0 P \exp(E/T) \tag{24c}$$

will fit the data[11,14] on η for TCP over the range −66 to 24 °C with $P = 0.095$, $E = 6280$ K, $\alpha^{-1} = 2335$ K, $T_0 = 153$ K, and $\log(A\zeta_0/Pa{\cdot}s) = -9.423$ (for a low molecular weight fluid, $\zeta = \eta/A$, with A a temperature-independent parameter). The parameters α^{-1} and T_0 are from ref 14. The form of eq 24 is empirical—we know of no simpler expression that will fit the data over the specified temperature range. With eq 24, the apparent activation energy $W = \partial \ln \zeta/\partial T^{-1}$ is E for large T and $\alpha^{-1}[T/(T - T_0)]^2$ for T near T_0. The appearance of a term related to free volume (ζ_{VOG}) and a term involving an activated process (ζ_{ACT}) appears necessary and reasonable to fit the data on TCP. For many polymer solutions, $T_g - T_0$ is about independent of ϕ, and the variation of α with ϕ is not large.[3] The possible dependence of ζ_{ACT} on ϕ has not been studied. In the following, we assume that ζ_{ACT} is independent of ϕ and that variation of ζ_{VOG} with ϕ is determined by free-volume considerations. This assumption is consistent with the sharp increase of W with increasing ϕ. The dependence of T_g on concentration is large if the T_g's of solvent and polymer differ markedly. For many solutions the Fox–Loshaek relation[3,15]

$$T_g^{-1} = (1 - w)T_{g^1}^{-1} + wT_{g^2}^{-1} \tag{25}$$

allows for interpolation between the glass transition temperatures T_{g^1} and T_{g^2} of solvent and solute, respectively, with w the solute weight fraction. A Taylor expansion of $\ln \zeta_{VOG}$ about w gives eq 4 to first-order, with

$$b_T = \left\{\frac{1}{\alpha(T - T_0)^2}\right\}\left[\frac{\partial T_g}{\partial w} - \frac{\partial \Delta}{\partial w}\right] - \frac{1}{\alpha^2(T - T_0)}\left\{\frac{\partial \alpha}{\partial w}\right\}_{w=0} \tag{26}$$

The data in Figure 10 show that b_T is 2.7-fold larger for solutions in TCP and DOP than the value $(b_T)_{CP}$ given in part 2 for solutions of polystyrene in cyclopentane at the same temperature and concentration range. This difference is reasonable since T_g is expected to be much reduced for the latter in comparison with that for TCP and DOP; the value of b_T for TCP solutions is consistent with eq 26 with very small to nil dependence of Δ and α on w using the values of α and T_0 given above. The data in Figure 10a also show that the first-order expansion is inadequate for $w >$ ca. 0.2. Retention of the next term in the Taylor expansion would add the term $k_T(b_T w)^2$ to $b_T w$ in eq 4. This modification with $k_T = 0.075$ will fit the data on $\eta_{rel}/\phi^{1/2}(\phi M_w)^{3.4}$ for solutions in DOP and TCP.

Since α-chloronaphthalene is a good solvent for polystyrene[23] and $c < c_s$ for the high molecular weight polymers used in figure 10b, $\eta_{rel}/\phi^{1/2}(\phi M_w)^{3.4}$ is proportional to $\phi^{-3.4s}\zeta(\phi)/\eta_s$. Assuming $\mu \approx 0.75$ (based on the estimate in ref 23), $s \approx 0.22$. Similar effects are suppressed for the data on solutions in aroclor shown in Figure 10b since $\mu \approx 0.64$ ($K = 0.51$ mL/g)[30] and $\phi^{1/2}\phi^{-3.4s}$ is essentially unity. Analysis of the data in Figure 10b give b_T about $2.3(b_T)_{CP}$ and $2.7(b_T)_{CP}$ for solution in α-chloronaphthalene and aroclor, respectively, with the latter being fitted for $w >$ 0.5 by inclusion of the term $0.075(b_T w)^2$ in eq 4.

Viscoelastic Behavior. The linear viscoelastic functions (e.g., $J(t)$, $R(t)$, $J^{(d)}(\omega)$, $J'(o)$, etc.) found for solutions of polystyrene in DOP at the Flory Θ temperature are

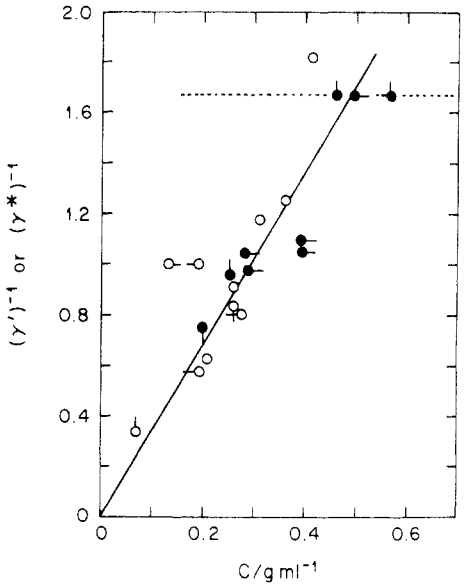

Figure 11. Inverse critical strain $(\gamma')^{-1}$ versus the volume fraction polymer ϕ for solutions of polystyrene and other polymers. The filled circles were obtained in this study for solutions of polystyrene from the strain at which $\eta^+(t,\kappa)$ deviates from $\eta^+(t,0)$, and the unfilled circles are estimates from the literature based on creep measurements.[11] For the former, the symbols designate PC3a in DOP at the Flory Θ temperature (pip up); PC3a in TCP (pip right); PC6a in TCP (pip down). The symbol designation for the unfilled circles is given in the original. The dashed line gives the "universal" value predicted theoretically.[9]

similar to those reported for solutions of polystyrene in TCP.[11] For example, $R_0^{(s)}/R_0^{(N)}$ is similar to the value reported for solutions in TCP,[11,14,21] showing that the breadth of the distribution of relaxation times is similar in the two cases. A discrete set of retardation times λ_i and weights r_i was determined for each solution in DOP from analysis of $R(t)$, and discrete sets of relaxation times τ_i and weights η_i were computed from these and the viscosity η_0, using methods given elsewhere[11]—the data on r_i, λ_i, η_i, and τ_i on the systems studied here are given in ref 31. The linear stress relaxation $\eta^-(t,0)$ computed as

$$\eta^-(t,0) = \sum \eta_i \exp(-t/\tau_i) \tag{27}$$

and the linear stress growth $\eta^+(t,0)$ during a ramp strain, which is related to $\eta^-(t,0)$ by the expression

$$\eta^+(t,0) = \eta_0 - \eta^-(t,0) \tag{28}$$

are well represented with the τ_i and η_i so obtained.

For solutions of polystyrene in TCP and a number of other systems, the onset of nonlinear viscoelastic behavior appears to occur when the strain in the sample exceeds a critical value γ', provided that at the same time the strain rate κ exceeds about τ_C^{-1}, where $\tau_C = R_0^{(s)}\eta_0$.[11] The strain at which $\sigma(t)/\kappa$ deviates from its low strain rate behavior in deformation at constant κ provides an estimate of γ'. Values obtained in that way are given in Figure 11, along with estimates reported elsewhere on the basis of creep behavior.[11] The results are in reasonable agreement, giving γ' inversely proportional to ϕ for $\phi < 0.5$, with $\gamma' \approx 0.6$ for larger ϕ. The latter value coincides with the γ' for which $F(|\gamma|)$ begins to exhibit significant departure from unity according to one theoretical treatment.[9] As in previous work, γ^+ is independent of ϕ. The data on $F(|\gamma|)$ for a solution of D-500 in DOP shown in Figure 5 are consistent with this behavior, giving $F(|\gamma|) \approx 1$ for $|\gamma| < \gamma'$ and and exponential decrease of $F(|\gamma|)$ with increasing $|\gamma|$ for larger $|\gamma|$, in accord with eq 19. Thus, it appears that the function $F(|\gamma|)$ in eq 7 to be used at the Flory Θ temperatures is identical with that used previously in analysis of data in good solvents.

As discussed elsewhere,[11,19] use of eq 19 in eq 4 for a ramp strain history ($\gamma(t) = \kappa t$ for $t > 0$) gives the result

$$\eta_\kappa = \sum \eta_i h(\beta\kappa\tau_i) \tag{29}$$

where $\beta^{-1} = \gamma''(1 + \alpha - \alpha^2/2)^{1/2}$, with $\alpha = \gamma'/\gamma''$. Inasmuch as α does not vary much and is small (<0.5), $h(\beta\kappa\tau_i)$ is nearly dependent on $\kappa\tau_i/\gamma''$. The expression

$$h(\beta\kappa\tau_i) = [1 + (\beta\kappa\tau_i)^\epsilon]^{-2/\epsilon} \tag{30}$$

with $\epsilon = {}^6/_5$ provides a useful approximation in most cases and illustrates the sharp decrease of $h(\beta\kappa\tau_i)$ as $\kappa\tau_i$ exceeds γ''. As mentioned elsewhere, comparison of eq 29 for η_κ with the linear functions given by eq 27 and

$$\eta^{(d)}(\omega) = [\eta'(\omega)^2 + \eta''(\omega)^2]^{1/2} \tag{31a}$$

$$\eta'(\omega) = \sum \eta_i g(\omega\tau_i) \tag{31b}$$

$$\eta''(\omega) = \sum \eta_i g(\omega\tau_i)(\omega\tau_i) \tag{31c}$$

where $g(\omega\tau_i) = [1 + (\omega\tau_i)^2]^{-1}$, provides a basis to understand the Cox–Merz relation $\eta_\kappa \approx [\eta^{(d)}(\omega)]_{\omega=\kappa}$, and the approximation $\eta_\kappa \approx [\eta^-(t,0)]_{\kappa t=1}$. Comparisons are given among these functions for data obtained on solutions of PC3a and D-500 in DOP in Figures 7 and 8. The reduced variables $x\eta_0/w^2$, with $x = \omega$, κ, or t^{-1} are proportional to $x\tau_C$ given the behavior in Figure 9. The resultant superposition seen in Figures 7 and 8 obtains since the τ_i/τ_C are independent of T and only weakly dependent of ϕ. The results obtained here reveal no unusual behavior at the Flory Θ temperature, with behavior that is quite similar to that in good solvents after proper scaling.

With use of eq 6 and 19, $\eta^-(t,\kappa)$ is given by

$$\eta^-(t,\kappa) = \sum \eta_i h(\beta\kappa\tau_i) \exp(-t/\tau_i) \tag{32}$$

Computations with the experimental η_i and τ_i show that for the solutions studied here, eq 32 may be expressed in the alternate form

$$\eta^-(t,\kappa) \approx \sum \eta_i \exp(-\hat{t}/\tau_i) \tag{33}$$

where $\hat{t} = t/\beta_\kappa$, with $\beta_\kappa \approx \tau_\kappa/\tau_C$. Here, τ_κ equal to $R_\kappa\eta_\kappa$, with R_κ the recoverable compliance following steady flow at shear rate κ, represents an average over the τ_i in steady flow at shear rate κ, given by

$$\tau_\kappa = \tau_C \frac{\sum \eta_i\tau_i\{1 - [1 - h(\beta\kappa\tau_i)] \exp(-\tau_\kappa/\tau_i)\}}{\sum \eta_i\tau_i} \tag{34}$$

(τ_κ tends to τ_C for $\kappa\tau_C < 1$). Equation 33 is the form found empirically for $\eta^-(t,\kappa)$ in this study—similar behavior has been found with other systems.[32]

Conclusions

The linear and nonlinear viscoelastic properties determined for moderately concentrated solutions of polystyrene at the Flory Θ temperature exhibit no unexpected behavior vis-à-vis corresponding solutions in a good solvent. The differences between the two vanish as the solution in a good solvent exceeds a concentration c_s, where c_s is the concentration for which $\alpha_C = 1$ (see eq 4). For smaller c_s, (net) repulsive binary interactions, which vanish at the Flory Θ temperature, affect chain dimensions in a good solvent, along with linear viscoelastic parameters such as η_0 and $R_0^{(s)}$. Nevertheless, properly normalized linear and nonlinear viscoelastic functions are similar in good solvents

and at the Flory Θ temperature, after normalization of the appropriate time scale by $\tau_C = \eta_0 R_0^{(s)}$.

Acknowledgment. This study, which was supported in part by a grant from the Polymers Program, Division of Materials Science, National Science Foundation, comprises part of the Ph.D. dissertation of J.O.P.

Registry No. Polystyrene, 9003-53-6.

References and Notes

(1) Berry, G. C. *J. Chem. Phys.* **1967**, *46*, 1338.
(2) Hager, B. L.; Berry, G. C. *J. Polym. Sci., Polym. Phys. Ed.* **1982**, *20*, 211.
(3) Berry, G. C.; Fox, T. G *Adv. Polym. Sci.* **1968**, *5*, 261.
(4) Grasseley, W. W. *Adv. Polym. Sci.* **1974**, *16*, 1.
(5) Casassa, E. F.; Berry, G. C. In *Comprehensive Polymer Science*; Booth, C., Price, C. Eds.; Pergamon Press: Oxford, 1988; Vol. 2, Chapter 3.
(6) Daoud, M.; Cotton, J. P.; Farnoux, B.; Jannink, G.; Sarma, G.; Benoit, H.; Duplessix, R.; Picot, C.; de Gennes, P.-G. *Macromolecules* **1975**, *8*, 804.
(7) Berry, G. C. In *Encyclopedia of Polymers Science and Engineering*; Mark, H., Overberger, C. G., et al., Eds.; Wiley: New York, 1987; Vol. 8, p 721.
(8) Muthukumar, M.; Edwards, S. F. *Polymer* **1982**, *23*, 345.
(9) Doi, M.; Edwards, S. F. *The Theory of Polymer Dynamics*; Clarendon Press: Oxford, 1987; Chapter 7.
(10) Doi, M. *J. Polym. Sci., Polym. Phys. Ed.* **1983**, *21*, 667.
(11) Nakamura, K.; Wong, C.-P.; Berry, G. C. *J. Polym. Sci., Polym. Phys. Ed.* **1984**, *22*, 1119.
(12) Bernstein, B.; Kearsley, E. A.; Zappas, L. J. *Trans. Soc. Rheol.* **1963**, *7*, 391.
(13) Ferry, J. D. *Viscoelastic Properties of Polymers*, 3rd. ed.; Wiley: New York, 1980; Chapter 1.
(14) Riande, E.; Markovitz, H.; Plazek, D. J.; Raghupathi, N. *J. Polym. Sci., Symp. No. 50* **1975**, 405.
(15) Fox, T. G; Loshaek, S. *J. Polym. Sci.* **1955**, *15*, 371.
(16) Berry, G. C.; Birnboim, M. H.; Park, J. O.; Meitz, D. W.; Plazek, D. J. *J. Polym. Sci., Part B*, in press.
(17) Birnboim, M. H.; Burke, J. S.; Anderson, R. L. In *Proc. Fifth Int. Congr. Rheol.*; Onogi, S., Ed.; University of Tokyo Press: Tokyo, 1969; Vol. 1, p 409.
(18) Riande, E.; Markovitz, H. *J. Polym. Sci., Polym. Phys. Ed.* **1975**, *13*, 947.
(19) Berry, G. C.; Plazek, D. J. In *Glass: Science and Technology*; Uhlmann, D. R., Kreidl, N. J., Eds.; Academic Press: New York, 1986; Chapter 6.
(20) Markovitz, H. In *Physics Vade Mecum*; Anderson, H. L., Ed.; Institute of Physics: New York; p 274.
(21) Plazek, D. J.; Riande, E.; Markovitz, H.; Raghupathi, N. *J. Polym. Sci., Polym. Phys. Ed.* **1979**, *17*, 2189.
(22) Plazek, D. J., private communication.
(23) (a) Takahashi, Y.; Noda, I.; Nagasawa, M. *Macromolecules* **1985**, *18*, 2220. (b) Takahashi, Y.; Umeda, M.; Noda, I. *Macromolecules* **1988**, *21*, 2257.
(24) Cox, W. P.; Merz, B. H. *J. Polym. Sci.* **1958**, *28*, 619.
(25) Kusamizu, S.; Holmes, L. A.; Moore, A. A.; Ferry, J. D. *Trans. Soc. Rheol.* **1968**, *12*, 559.
(26) Einaga, Y.; Osaki, K.; Kurata, M.; Tamura, M. *Macromolecules* **1971**, *4*, 87.
(27) de Gennes, P.-G. *Scaling Concepts in Polymer Physics*; Cornell University Press: Ithaca, NY, 1979; Chapter 8.
(28) Yamakawa, H. *Modern Theory of Polymer Solutions*; Harper & Row: New York, 1971; Chapter 7.
(29) Kulicke, W.-M.; Kniewske, R. *Rheol. Acta* **1984**, *23*, 75.
(30) Bueche, B. *Physical Properties of Polymers*: Interscience: New York, 1962; Chapter 5.
(31) Park, J. O. Ph.D. Thesis, Carnegie-Mellon University, 1986.
(32) Venkatraman, S.; Berry, G. C.; Einaga, Y. *J. Polym. Sci., Polym. Phys. Ed.* **1985**, *23*, 1275.

Solvation Effect upon Glass Transition Temperature and Conductivity of Poly(ethylene oxide) Complexed with Alkali Thiocyanates

S. Besner and J. Prud'homme*

Department of Chemistry, University of Montreal, Montreal, Quebec, Canada H3C 3V1.
Received July 26, 1988; Revised Manuscript Received December 12, 1988

ABSTRACT: The apparent solvation numbers, SN, of LiSCN, KSCN, and CsSCN in amorphous poly(ethylene oxide) (PEO) have been inferred from the salt saturation concentrations in melt-quenched amorphous mixtures. On an EO unit molar basis, these numbers are EO/Li = 3, EO/K = 4.9, and EO/Cs = 9. They increase linearly with the cation atomic surfaces and, when extrapolated to zero atomic surface value, they yield an apparent solvation number of 2 for the thiocyanate anions. In turn, the apparent coordination numbers, CN, of the alkali cations with respect to the EO units are given by the relation CN = SN − 2. The glass transition temperature (T_g) dependence upon the salt molar concentration is the same for the three systems, suggesting that the cation–EO binding energy is inversely proportional to CN. More surprising is that for the molar ratio EO/M = 8, for which the ac conductivity of amorphous mixtures of the three systems could be investigated in the temperature range 10–100 °C, conductivity magnitude at reduced temperatures $T - T_g$ is directly proportional to CN. This straightforward correlation is interpreted in terms of an ionic structure in the concentrated regime that would consist of ions surrounded by an ion atmosphere of opposite sign. Conduction appears to occur through an exchange of solvating EO units at a rate determined by both the segmental motion of the PEO chains and the cation–EO binding energy. Ion–ion interactions are also important as judged by a decrease of conductivity magnitude with increasing salt concentration for the PEO–LiSCN system.

Introduction

In a recent paper,[1] we reported a complete phase diagram for the PEO–NaSCN system (PEO = poly(ethylene oxide)) together with a partial phase diagram for the PEO–KSCN system. In each case the phase diagram was constructed by means of DSC measurements performed on solvent-cast mixtures prepared with a low molecular weight PEO sample ($M_n = 4 \times 10^3$), in order to avoid entanglement effect upon crystallinity. In spite of this concern, it turned out that only the mixtures with NaSCN were highly crystalline over the entire composition range. Those with KSCN exhibited a crystallinity gap in the range of the PEO-rich compositions. The phase diagrams of the PEO–NaSCN and PEO–KSCN systems show great similarities. Each involves an intermediate crystalline compound, $P(EO_3{\cdot}NaSCN)$ or $P(EO_{\sim 4}{\cdot}KSCN)$, that melts incongruently (at 182 or 95 °C) to yield the solid salt. Above the melting temperature of the intermediate compound, the solubility curve of each salt is nearly vertical. Also, in each case the same solubility limit as that defined

0024-9297/89/2222-3029$01.50/0